Removal of Bacillus spores from stainless steel pipes by flow foam: Effect of the foam quality and velocity

Ahmad Al Saabi, Heni Dallagi, Fethi Aloui, Christine Faille, Gaétan Rauwel, Laurent Wauquier, Laurent Bouvier, Thierry Benezech

Paper entitled:

Removal of *Bacillus* spores from stainless steel pipes by flow foam: effect of the foam quality and velocity

Authors and affiliation :

Ahmad Al Saabi [1], Heni Dallagi [1], Fehti Aloui[2], Christine Faille [1], Gaétan Rauwel[3], Laurent Wauquier[1], Laurent Bouvier[1] and Thierry Bénézech [1,*]

[1] Univ. Lille, CNRS, INRAE, ENSCL, UMET, F-59650, Villeneuve d'Ascq, France ; ahmad.al-saabi@inrae.fr; heni.dallagi@inrae.fr; christine.faille@inrae.fr; laurent.wauquier@inrae.fr; laurent.bouvier@inrae.fr

[2] Polytechnic University Hauts-de-France, LAMIH CNRS UMR 8201, Campus Mont-Houy, F-59313 Valenciennes Cedex 9, France ; Fethi.Aloui@uphf.fr

[3] Anios-Ecolab, Sainghin-en-Mélantois, France ; gaetan.rauwel@anios.com

* Correspondence: Thierry.benezech@inrae.fr

1. Introduction

In agro-food industrial environments, surfaces have been reported to be contaminated by a range of microorganisms, including pathogenic and spoilage bacteria (Srey et al., 2013). Once introduced, if environmental conditions are suitable, many bacteria are able to persist on the contaminated surfaces or even to form biofilms. Indeed, despite cleaning and disinfection procedures, some bacteria are still commonly found on the surfaces of food processing lines, mostly in the form of adherent spores, e.g. *Bacillus* spores in closed equipment(Peng et al., 2002) or in the form of biofilms, e.g. *Pseudomonas spp*.(Dogan and Boor, 2003).

Cleaning in place (CIP) leading to residue removal from inner surfaces of processing lines without disassembling, has been a crucial factor in guaranteeing the safety and quality of food. If not done properly, consequences can be devastating, especially in the case of pathogen surface contamination (Pietrysiak et al., 2019; Ribeiro et al., 2019). In order to clean rapidly, CIP aims to combine the advantages of the high temperature, detergent and the mechanical action generated by the turbulent flow (or the impact of the spray) (Moerman et al., 2014). The mechanical effect is created by the flow rate and it is generally admitted that high flow rates result in high removal rates because of the high shear forces on the deposit layer. However some works have detailed the role of hydrodynamics and in particular of the mean wall shear stress and the major role played by its fluctuations (Blel et al., 2013, 2010). This was very recently judged to be mandatory for any CIP improvement (Li et al., 2019).

The addition of foaming surfactants or even gas-stabilized foam means the cleaning solution can be applied as a foam, which can increase the retention time, e.g. on vertical surfaces. Foam is widely used in static conditions throughout the food industry for the cleaning of large open surfaces (floor, conveyors, workshops and equipment). To clean open surfaces, foam requires specific qualities, namely density, foamability, stability and void fraction-based quality. However, foam cleaning agents could also be used for cleaning some closed equipment such as filtration modules (Gahleitner et al., 2013). Despite its widespread use, very little work has been carried out on the elimination of surface deposits using flowing foam, essentially gas-liquid two-phase flows in capillaries (Kondjoyan et al., 2009) and to our knowledge none have dealt with the elimination of microorganisms.

Almost nothing is known about the potential of foam flow to conduct cleaning operations using much less energy (very low velocity) and much less water. Aqueous foams are non-Newtonian complex fluids consisting of concentrated dispersions of gas bubbles in a soapy liquid. Depending on the amount of water they contain, they can be either wet or dry. The air fraction defines the so-called foam β quality (Tisné et al., 2004). Foams have original mechanical properties which rely on their low density and high surface area combined with their ability to elastically respond to low stresses and to flow like a viscous liquid with large distortions.

Foams admit an unexpected and nonlinear rheological behavior (shear thinning and yielding), where the properties of the liquid and gas, that compose it, have an influence on it. Their rheological behavior can be compared with some non-Newtonian models such as, power law, Bingham, and Herschel–Bulkley. Recently it was demonstrated that the foam rheological behavior can be better described by Herschel-Bulkley model (Dallagi et al., 2019, 2018).

Among the consequences of foam flow, the mechanical action exerted on the contact-surface depends on the velocity, foam composition (air/liquid) and the ability of the system (foam, geometry and surface properties of the equipment to be cleaned) to maintain a thin liquid film between the solid surface (wall) and the foam flow.

Wall shear stress, especially due to this thin liquid film located between the wall and the foam flow, plays an important role in the characterization of the rheological properties of this foam, depending mainly on the bubble size and particularly on the volume fraction of the liquid (Chovet, 2015; Chovet et al., 2014). These properties can be used to understand the microorganism detachment phenomena, such as spores from solid surfaces. Therefore, foam flows would constitute a true novelty in surface hygiene, as low water load and high mechanical actions under moderate temperatures would permit highly cleaning, which can easily be combined with disinfection.

This study investigates the removal kinetics of *B. amyloliquefaciens* 98/7 and *B. cereus* 98/4 spores using foam flow. The respective roles of the foam quality (importance of air/water balance), and of the flow rate were analyzed by means removal kinetics modeling. Results were then compared to spore removal under mild cleaning in place conditions. We then investigated some foam properties (the flow regime and the mean foam flow velocity,

bubble-size distribution, bubble-passage frequency, foam quality and mean wall shear stress).

2. Materials and Methods

2.1. Bacterial strains and solid surfaces

In this study, two bacterial strains isolated from dairy processing lines forming spores of very different surface energies one hydrophobic and the second hydrophilic (Faille et al., 2019, 2016, 2010) were used: *B. cereus* CUETM 98/4 (BC-98/4) and *B. amylolichefaciens* CUETM 98/7 (formerly known as *B. subtilis* 98/7). *Bacillus* spores were produced as previously described (Faille et al., 2019). Before any experiment, two further washes were performed and spores were subjected to a 2.5-min ultra-sonication step in an ultrasonic cleaner (Bransonic 2510E-MT, 42 kHz, 100 W, Branson Ultrasonics Corpo-ration, USA) to limit the presence of aggregates. In order to evaluate the hydrophobic character of spores, Microbial Affinity to Hydrocarbons tests (MATH) were performed as previously described (Faille et al., 2019b).

The material, used in the form of rectangular coupons (45 mm x 15 mm), was AISI 316 stainless steel with pickled (2B) finish (kindly provided by APERAM, Isbergues, France). Prior to each experiment, coupons were cleaned and disinfected using a standard protocol used at UMET. Coupons was first cleaned using pure alkaline detergent (RBS T105, Traitements Chimiques des Surfaces, France). They were then subjected to a 10 min immersion in a 5% RBS T105 at 60 °C, followed by thorough rinsing with tap water, then with softened (reverse osmosis) water for 5 min each. 24 h before the experiments, stainless steel coupons were treated in a dry heat oven at 180°C for 1 h.

2.2. Surface soiling and cleaning

The soiling suspensions were prepared with ultra-purified sterilized water and a spore concentration of around 10^6 CFU/ml. The coupons were vertically immersed in a Beaker containing 250 ml of the soiling solution, then kept at room temperature for 4 hrs.

Coupons were then inserted into a 23 10^{-2} m long stainless steel test duct with a 1.5 x 1 10^{-2} m rectangular cross-section. The geometry of the rectangular test ducts used for the

93 experiments was previously described (Cunault et al., 2015). The three central coupons out
94 of the five installed in the ducts were soiled and further analyzed after cleaning.
95 The production foam prototype was built according to previous work (Chovet and Aloui,
96 2016; Tisné et al., 2003a). The experimental set-up, with an open foam flow circuit, was
97 designed to allow the foam flow to develop within horizontally-placed square ducts, with
98 the coupons to be cleaned at the top. The test ducts were situated after a transparent
99 Plexiglas rectangular duct, of identical inner size,to visualize the foam flow. To allow steady
100 state flow conditions, the test ducts were placed at intervals exceeding 80 times the
101 hydraulic diameter of the vein inlet (i.e. 1.5 m).
102 The prototype is presented in Figure 1. The rig includes a mother tank (capacity: 100 L)
103 filled with Sodium Dodecyl Sulfate (Sigma-Aldrich ReagentPlus®, over 98.5% purity)
104 dissolved in osmosed water (0.15% ww). The SDS solution is pumped into the feeding tank
105 (50 L) located at a height of 3 m using a positive displacement pump (VARMECA 21TL055,
106 Leroy-Somer). This set-up creates a constant flow rate in the foam generators due to gravity.
107 Three foam generators were designed as previously described (Tisné et al., 2003a).
108 The foam is generated by injection of pressurized air through a porous medium (DURAN®,
109 pore sizes ranging from 1 to 1.6 µm, Dislab, Lens, France), inside cylindrical containers filled
110 with the SDS solution. The foam quality describing the air/water content of the foam was
111 calculated as follows (Equation 1) according to (Chovet and Aloui, 2016) where Q_g and Q_l
112 are respectively the gas and liquid flow rates:
113 .
114
115 $$\beta = \frac{Qg}{Qg+Ql} \qquad (1)$$
116
117 The three independent parallel generators allowed us to increase the bulk velocity
118 without affecting the foam structure. Three foam qualities were chosen for the cleaning
119 experiments 50%, 60% and 70%. The mean velocity was calculated taking into account the
120 global flow rate (Q_l+Q_g) divided by the cross-section area S of the test duct. The Reynolds
121 number was calculated according to Equations (2) and (3), taking into account the density
122 of both gas and liquid phases. Foam viscosity was calculated using the relationship based
123 on a heuristic model of concentrated emulsions (Equation 4).
124

$$Re = \frac{\rho_f . \bar{v} . d_h}{\mu_f} \quad (2)$$

$$\rho_f = (1 - \beta) . \rho_l + \beta . \rho_g \quad (3)$$

$$\mu_f = \frac{\mu_l}{1 - \mu_l{}^{1/3}} \quad (4)$$

Three liquid/air flowmeters enabled the adjustment of the flow rate from 0 to 35 l h^{-1} and 0 to 70 l h^{-1} respectively.

Flowing from the generators, the foam passes through a transparent Plexiglas pipe of 1.1 m length. The transparent pipe enables the visualization of the foam texture, bubble size and foam velocity measurement. Two pressure outlets allow the connection of 2 manifold tubes placed over a scaled plate that measures on a length L of 1m the pressure drop ΔP to calculate the mean wall shear stress $\bar{\tau}$ (d_h ΔP / 4 L). For each cleaning experiment, only one test duct containing the soiled coupons was clamped to the transparent pipe.

The different test ducts were thus cleaned with three foam qualities at 20°C, at foam mean velocities ranging from 2.1 to 6.7 m s-1, for 15 and 35 s, 1, 3, 5, 10 and 20 min and other experiments were carried out to mimic CIP conditions. The test ducts were connected to a CIP pilot rig (Jullien et al., 2008) and a simple CIP procedure was then carried out under the same conditions as those used for the foam tests, i.e. SDS concentration, temperature, cleaning times. The flow rate was selected to generate a mean wall shear stress of 5 Pa, falling within the range of the mean wall shear stress conditions induced by the flowing foam as described in the Results Section. After the cleaning process, the coupons were removed from the test tubes and rinsed by dipping in a beaker containing one liter of sterile ultrapure water. The residual spore contamination was then analyzed as follows.

To determine the number of adhering spores before (N0) or after the (Nresid) cleaning procedure, coupons were subjected to an ultrasonication step in 10 ml of 2% Tween 80 (v/v) in peptone water without indole 0.015 g/L (Biokar), diluted to 1L with ultra-purified sterilized water (5 min, Ultrasonic bath, Branson 2510, 40 Hz). This treatment has been previously shown, in our laboratory, to remove more than 99% of the adherent spores (Tauveron et al., 2006). The detached spores were enumerated on nutrient agar composed

of 1.3% w/v nutrient broth (Biorad, France) and 1.5% w/v bacteriological agar type E (Biokar Diagnostics, France) after 48 h at 30°C. The percentage of residual spores after cleaning was then calculated [(Nresid/N0) * 100].

For microstructure examination, some rinsed coupons were first dried at 20 °C for at least 1 hour to prevent spore detachment during the staining procedure. The coupons were then stained with orange acridine (0.01%) for 15 min at 20°C, gently rinsed with softened water and allowed to dry before observation. Finally, the surface contamination organization was observed using an epifluorescence microscope (Zeiss Axioskop 2 Plus, Oberkochen, Germany) at magnification 1000X.

2.3. Foam flow visualisation

The method is based on the observation of the displacement of moving bubbles at the walls of the pipe, for a given interval. In situ measurements were carried out at the last part of the pipe where the foam flow could be considered as established. The velocity of the bubbles was measured by marking the Plexiglas pipe wall by two thin marks spaced at a known distance. For both the lateral and the top walls of the pipe, three locations were chosen: two at 1 mm from the edges and one in the middle of the observed wall. The time taken for a bubble to pass between the two marks was recorded to calculate the its velocity. The smallest easily-visible bubbles (0.3 mm) were considered for tracking and 10 successive measurements were carried out. Mean values were then calculated. These could be considered as representative of the local velocity at the wall whatever the bubble size (Tisné et al., 2003). This method gives an approximation of the bubbles' speed. A selection of photos of the foam flow (camera Panasonic LUMIX DMC-FZ62, High speed video [HS], at a speed of up to 200 frames / second) were analyzed using Piximètre 5.1 R1540 image analysis software. The clearest two images in terms for each flow condition induced by the generators and for the three foam qualities were filtered to better observe the borders of the bubbles. It was thus possible to evaluate the bubble size distribution in all the cases studied.

An optical probe (© RBI instrumentation, Meylan, France) based on the discrete variation of the refractive indicator optics between the two-phase flow (air/liquid) was used to evaluate the void fraction and the air bubbles' passage frequency at the wall top (at 0.5 mm from the top). Data were analysed using the ISO software provided by RBI.

2.4. Kinetics modelling

A two-phase kinetics model was used to fit the data as previously proposed for the detachment kinetics of biofilms during CIP (Benezech and Faille, 2018). The fitting was performed using GInaFIT (Geeraerd et al., 2005) using a biphasic model composed of two first order kinetics (Dallagi et al., 2018b, 2019).

2.5. Statistical analysis

At least 3 repetitions were carried out for the quantitative analysis of the residual contamination after foam cleaning. Data were analysed by general linear model procedures using SAS V8.0 software (SAS Institute, Gary, NC, USA). Variance analysis was performed to determine how the bacteria removal described by the kinetic parameters (residual contamination at different cleaning times and model parameters were affected by the cleaning conditions tested .

3. Results

3.1. Foam flow organization and mechanical action induced by the foam

Three foam qualities were prepared with a concentration of SDS of 0.15 % w/w in order to exceed the Critical Micelle Concentration (CMC). The SDS as an anionic surfactant is a good representative of the “sulphate” surfactants largely used in formulated detergents. The SDS is known to be highly soluble and easy to rinse and is largely used in academic studies (Mai et al., 2016). Anionic surfactants are recognized for their cleaning, foaming and emulsifying properties. The foam generated was found to be very stable (no changes were observed in terms of foam drainage and bubble size over one hour – data not shown). We also checked that the use of one, two or three generators in parallel failed to modify the foam structure significantly, despite the differences in the foam velocity. Thanks to the transparent Plexiglas tube, placed upstream of the test duct with the soiled coupons subjected to the cleaning procedure, it was possible to visualise the foam flow through the rig and to take images or videos. Observations were made from one side and from through the top.

The bubble velocity was first measured as shown in Figure 2 in three locations on each selected duct wall (top and lateral). As shown in Figure 2, depending on the experimental conditions (number of generators, foam quality), the velocity profiles were quite different. As the mean velocity increased, a difference in the flow velocity of the bubbles appeared depending on their position in the duct. Indeed, when a single generator was used, bubble velocity was generally constant and the foam flow therefore behaved like a plug flow. The increase induced by two generators showed no change at the top of the duct, except for the foam quality of 70%. Conversely, the bubble velocities increased from the top to the bottom of the duct as shown in Figure 2 B. This is due especially to the underlying liquid film, which pulls the foam in contact because its velocity increases. At the top wall, bubble velocities were highest at the centre of the side, and thus decreased as the flow approached the duct edges. All conditions used are summarized in Table 1.

The foams' flow conditions varied from 2.0 to 8.6 cm s^{-1}, whilst for the CIP conditions the velocity was significantly higher at 120 cm s^{-1} and the flow regime was turbulent (Re > 14500). The mean wall shear stress (WSS) condition for the CIP was chosen to fall within those induced by the foam, i.e. ranging from 2.2 to 6.4 Pa, allowing comparison between the CIP mechanical action and the use of foam flow. One can note that the plug flow regime with constant foam velocity profile corresponding to 1 generator flow (all foam qualities) related to a Reynolds number maximum of 67. At over 100, the foam flow velocity profile at the top wall could not be considered as constant (Figure 2A).

In Figure 3, an example of photos of the foam flow arrangement at the top surface of the transparent duct is shown.

In order to identify the distribution of bubble size within the foam under different conditions, photos were taken at the top wall of the Plexiglas duct (Figure 3). The size distribution appeared to be affected by both velocity and foam quality. For example, the greater the velocity at the top wall, the smaller the bubbles.

The bubble sizes were then measured and the data are given in Figure 4. When only one generator was used, the bubble sizes were more heterogeneous than those obtained with two or three generators, whatever the foam quality. Moreover, a significant number of big bubbles (between 1 mm and 10 mm in size) was also observed. The increase in the velocity was thus more conducive to smaller bubbles. In accordance with Figure 3, some larger

bubbles (size > 1mm) could still be measured with 2 and 3 generators for the foam flow where β = 50% and with 2 generators for the foam flow where β = 60%.

The mean frequencies of the bubbles' passage observed by the optical probe (Figure 4, D) near the top wall increased with the number of generators. However, this increase could not be explained solely by the mean velocity, but is apparently also linked to the reduction in the bubble sizes e.g. for the foam 50%, the doubling or the tripling of the mean velocity induced an increase in the frequency by factors of respectively 2.9 and 7.1.

3.2. Spores' detachment under the different flowing conditions

Spore adhesion to the stainless steel coupons was 5.6 ± 0.4 log CFU cm^{-2} for *B. amyloliquefaciens* and 5.4 ± 0.3 log CFU cm^{-2} for *B. cereus*. Before any detachment experiments, we checked that spore incubation in SDS 0.15% did not result in any significant viability loss (data not shown). The detachment of *B. amyloliquefaciens* spores was investigated under all the flow conditions with each of the three foam qualities. In Figure 5, only the mean values of the remaining contamination at the different kinetic times were presented. In all cases, the detachment curves clearly showed two distinct phases.

Both phases appeared to be exponential and therefore were quite accurately described by the biphasic model, with R2 ranging from 0.62 to 0.98 and mostly over 0.80.

During the first detachment phase (less than 1 min), the spore detachment was very fast, with a 0.6 to 1.8 log decrease in the population of surface-attached spores. Large differences were observed according to the number of generators used with the 50%, foam quality whereas the number of generators had little effect on the detachment of the other two foams (60% and 70%). Taking into account all the conditions used, it appears that spore detachment during this first phase was much more efficient with the 50% foam quality when 1 or 2 generators were used. After this first step, the detachment continued for at least 20 minutes, i.e. the duration of the cleaning procedure, though more slowly. Here again, the spore detachment rate seemed dependent on the experimental conditions (number of generators, foam quality). The cleaning kinetics with foam were compared to a CIP using the SDS 0.15% and a mean wall shear stress of 5 Pa (Figure 5D). The first detachment step was close to the most efficient one with foam, i.e. allowing the detachment of over 1.5 log CFU, close to the one observed when 1 or 2 generators were

used with the β = 50% foam. Conversely, no further detachment occurred after this first phase, indicating that a plateau value had been reached.

The decimal reduction at 20 min, i.e. the end of the second phase of the cleaning kinetics, was statistically analysed to compare the role of the flow rates conditions induced by the generators, the different foam qualities and by the CIP conditions. At 20 min, cleaning efficiencies observed were comparable between CIP and the flow rates induced by one and two generators (letter A, Tukey's grouping) as shown in Figure 6. In addition, the cleaning efficiency induced by the 50% and 60% foam qualities appeared significantly better than the 70% foam (different letters according to the Tukey's grouping).

Focusing on the cleaning conditions with foam, the variance analysis confirmed that the variability observed on the three kinetics parameters (f, kmax1, and kmax2), was significantly related to the flow rate induced by the foam generators. However, some discrepancies should be noted (see Figure 7). Considering the potential combined effects of the foam quality and the flow rate (one, two and three generators) on the parameter f (f is the poorly adherent fraction of the population and/or less resistant to detachment), the variance analysis gave a p value of 0.027. The Tukey's grouping as shown in Figure 7, highlighted a slight effect of the flow rate: f being higher under the lowest flow rate conditions and higher with the foam where β=50%, compared to the foam with β=70% (no common letters, Tukey's grouping). More visible was the role of the flow rate on the constant rate Kmax1 (p=0.001), the lowest flow rate clearly being the most efficient condition for spore removal under this first phase: Kmax1 was multiplied by a factor up to 300. Foam quality appeared to play a role as the Tukey's grouping highlighted that Kmax1 values for the β=70% foam were very low compared to 50% and 60% foams. While taking into account data obtained with the CIP conditions, as also shown in Figure 7, flow conditions were still highly significant (P=0.0012) and three classes were defined by Tukey's grouping (A, AB and B). In this case, CIP conditions gave an intermediate mean value of 55 for Kmax1 compared to 87 with one generator and 6.7 or 1.3 respectively for two or

The effect of cleaning using foam flow, was tested with another *Bacillus* species. In Figure 8 the two kinetics appeared very similar with a quick detachment in less than one min followed by a second phase, with about 0.5 log removal in both cases. Such a cleaning condition was chosen as the most efficient, according to the results described above. The main difference lied in the Kmax1 values, *B. cereus* spores being more difficult to remove

than *B. amyloliquefaciens* ones at the initial phase of the kinetics. Conversely, the removal during the second phase of the kinetics appeared very similar and this was confirmed by close values of the detachment rate Kmax2 for the two bacteria.

The microscopic observations showed the spores distribution on the coupons before and at different cleaning times. Only times 0 (fouling), 15 s, 3 minutes and 20 minutes were considered for comparison between foam cleanings (0.5 and 1 generator), one of the most effective foam cleanings observed and CIP. Microscopic observation showed that *B. amyloliquefaciens 98/7* spores formed some clusters as shown in Figure 8, but these spores were mainly evenly distributed on the steel surface after the 4 hours soiling. Clusters were limited by the sonication of the spore suspensions prior to the soiling step and these were rapidly removed after only 15 s by both CIP and foam flow. Yet, according to Figure 9, removal was visibly greater with foam flow than CIP. The difference observed here (almost one log) is less than the one given by the removal kinetics (Figure 5B; 0.5 log difference), which considers viable and cultivable bacteria. However, the variability (up to 0.5 log) between trials could easily explain this discrepancy.

4. Discussion

Foam is a two-phase gas-liquid fluid, in which gas is the dispersed phase and liquid is the continuous phase, where the volume of gas greater than that of liquid. In this work, only wet foam was used, meaning that foam is formed only of spherical bubbles, as observed at the top wall as previously described (Chovet and Aloui, 2016; Tisné et al., 2004) . Each mean velocity induced by one, two or three generators engendered a different flow regime. Indeed, for the lowest mean velocity, the axial component was uniform over the entire cross-section, thereby corresponding to the mono-dimensional flow regime or plug foam flow regime. For the mean velocity of 4 cm s^{-1}, the flow appeared partially sheared with a sliding at the walls, the axial velocity component no longer being uniform, depending on the ordinate and corresponding to the two-dimensional (2D) foam flow regime. One can notice that the top wall velocity remained constant (foam at β=50% and β=60%) or was only slightly modified at the center of the top wall (foam at β=70%) under our experimental conditions. For the highest mean velocities, the foam flow was completely sheared with a sliding at the walls and could therefore be considered as three-dimensional (3D), with the underlying liquid film at the bottom of the duct flowing at a higher velocity, pulling the foam

344 flow above and therefore inducing a significant increase in the bubbles' velocity directly in
345 contact with this thick liquid film. This phenomenon is accompanied by a rearrangement of
346 bubble sizes, with the largest bubbles being mostly moved up the pipe. Such a phenomenon
347 was already described by (Tisné et al., 2003). In this work, the cleaning of surfaces by the
348 foam was evaluated at the top wall as a first evaluation of the role of flowing foam in the
349 removal of surface contaminations (bacteria spores). In parallel, even if the experimental
350 conditions were supposed to maintain the foam structure with the increase in the mean
351 velocity, it appeared that the bubble size repartition at the top wall varied with the foam
352 quality tested, meaning that bubble rearrangementhad occurred: the increase in the mean
353 velocity induced a reduction in the bubble size at the top wall.

354 Furthermore, it has been demonstrated that the variation at the top wall of the the thin
355 liquid film between the bubbles and the wall is directly affected by the bubbles passage and
356 depends on their size (Tisné et al., 2004), which could have an effect on the effectiveness
357 of adherent bacteria removal. The thickness fluctuations thus induced under their
358 experimental 1D flow conditions varied between 5 µm and 35 µm with a foam quality of
359 70%. Under 1D flow conditions for a foam quality of 55%, conditions close to our
360 experimental conditions Chovet and Aloui, 2016 , observed fluctuations at the top of the
361 channel liquid film varying from 2 µm to 40 µm. In addition, this amplitude decreased with
362 the increase in the foam quality, probably due to a change in the bubble size arrangement
363 at the wall.

364 Microscopic scale studies (Tisné et al., 2004), reveal that it is possible to rely on studies
365 of bubble flows inside circular capillaries, which will help in understanding the underlying
366 phenomena (Bretherton, 1961). Assuming that there was no tangential shear stress at the
367 fluid–fluid interface, he predicted that the film thickness was dependent on four
368 parameters: the tube radius r, the liquid viscosity μ_L, the surface tension γ and the bubbles'
369 velocity V_b. The film thickness is as follows:

370 $$e = 1.337\ r\ Ca^{2/3} \quad (5)$$

371 where Ca represents the capillary number defined as:

372 $$Ca = \mu_L\ V_b / \gamma \quad (6)$$

373 In relation to Bretherton's approach, r was assimilated to the radius of the bubble. Tisné
374 et al., 2004 representing the evolution of the measured contact film thickness versus $Ca^{2/3}$
375 observed a close agreement with the Bretherton law (Bretherton, 1961), the bubble size

considered being 0.5 mm. Our experiments are in a capillary number range of 11 10^{-4} < Ca < 44 10^{-4} (0.011 < $Ca^{2/3}$ < 0.026) falling within the range proposed by these authors, 3.10^{-4} < Ca < 28.10^{-4} (0.005< $Ca^{2/3}$ < 0.02). Given the agreement observed with the Bretherton law, the contact liquid film thickness in our experimental conditions would have ranged from 7 to 18 µm given a mean bubble radius of 0.5 mm, the thinnest liquid films being observed at the lowest velocities. Such a range of variation is in agreement with previous works (Chovet and Aloui, 2016; Tisné et al., 2004).

In parallel, it was shown (Tisné et al., 2003) that the wall shear stress was lower in the liquid film between each bubble and the wall. The wall friction was especially concentrated at the two ends of the bubbles; the wall shear stress fluctuations' amplitude being linked to the bubble size. When compared with the spore detachment kinetics, the greatest detachment efficiency appeared to be obtained with larger bubble size, notably when their diameter exceeded 0.1 mm, as clearly observed with the foam qualities of 0.5 (1D and 2D foam flow conditions) and 60% (1D foam flow condition) during the first step. Under CIP conditions, the detachment rate appeared to be comparable to the best foam cleaning conditions tested for comparable mean WSS conditions. In both cases the cleaning agent was the SDS under cold conditions (20°C). Previous work (Faille et al., 2018), highlighted the significant role of the fluctuation in the local wall shear stress on the cleaning efficiency under CIP conditions. One can draw a parallel here with these previous observations (Chovet and Aloui, 2016; Tisné et al., 2003), as the presence of the WSS fluctuations induced by the foam at the top wall appeared to play a role in the detachment mechanism and was clearly visibly under the 1D flow regime. However, for the 70%, foam quality, larger sized bubbles were observed at the top wall, which failed to ensure cleaning efficiency. Conversely, the increase in foam velocity meant a re-arrangement of the bubble sizes at the top wall (smaller bubbles). This phenomenon appeared to be unfavorable for efficient cleaning, as despite an increase in mean WSS, fluctuation amplitude decreased. Local wall shear stress decreases dramatically while bubble passes and increases to a maximum between bubbles (Tisné et al., 2003). Therefore, the frequency of fluctuation of the local wall shear stress with large bubbles is less than the fluctuation with small bubbles but the amplitude is higher and would explain the differences in the spores' removal.

The kinetics of bacteria spore detachment in the different flow and foam quality conditions were investigated and modelled according to previous work (Benezech and

Faille, 2018) on biofilm removal under CIP conditions. An identical simple two-phase model was found to be suitable for describing biofilm removal kinetics. The first bacterial removal phase corresponded to a quick removal of biofilm matrix with embedded cells, while the second phase accounted for the removal of cells directly attached to the steel surface. For bacterial spores removed by foam flow, the mechanisms appeared to be totally different, as the bacteria were evenly distributed on the stainless steel surfaces with very few clusters. This is unlikely to explain the quick and strong removal at the very beginning of the cleaning (less than 1 min). The parameter f corresponding to the part of the spore's population easily affected by the foam flow appeared to be significantly higher at the lowest velocities and for the wettest foam (β=50%). This also corresponded to the highest values of the Kmax1 constant rate, i.e. the first phase of the removal kinetics. However, the second kinetic phase did not significantly improve the cleaning efficiency as a whole, whatever the conditions. For biofilms, it was observed that the chemical action contrarily to the mechanical action induced by the foam flow, was only involved in the first removal kinetic phase. The addition of chemicals such as NaOH during CIP conditions would largely improve this initial kinetics removal phase (Benezech and Faille, 2018). The difficulty in removing the remaining spores during the second phase of the kinetics was probably due to the stainless steel surface finish 2B used, which was proven to be less hygienic than other finishes, such as bright annealed 2R, as it presents boundary grains where spores can accumulate. The fluctuations in the liquid film thickness and/or of the wall shear stress appeared to impact the detachment phenomenon to a lesser extent.

A comparison with previous work on particles detachment by bubbles moving in a capillary duct, will allow the potential role of the capillary forces in the bacterial detachment to be taken into account. Two types of particles in terms of surface energy (hydrophobic and hydrophilic) of a size comparable to the Bacillus spores were used (Kondjoyan et al., 2009b), the entire air–liquid interface was modelled and the time-variation of the capillary force during transit of the bubble at the surface was determined. The particle detachment curve was thus predicted from near zero velocity to the highest velocity value, at which capillary force was supposed to vanish.

The approach was validated using latex particles 2µm in diameter. The bell-shaped detachment curves experimentally obtained showed a width dependent on the value of the contact angle of the particles, the curve being narrower for hydrophilic particles than for

hydrophobic ones. The effective contact angle values of the particles could thus be deduced directly from the width of the detachment curves. *Bacillus amyloliquefaciens* 98/7 spores according to previous work were highly hydrophilic (Faille et al., 2010) with a contact angle to water of 20.5° (data not shown). For hydrophilic particles (Kondjoyan et al., 2009b), the detachment occurred at bubble velocities of around 3 cm s^{-1} and dramatically decreased at 5 cm s^{-1}. As far as a direct comparison is conceivable, such a velocity range corresponded to the variation range (2.2 – 5 cm s^{-1}), where the greatest detachment rate was observed, as illustrated by high Kmax1 constant rate values under 1D flow conditions. For hydrophobic particles, the bell-shaped detachment rate was wider and detachment started at greater bubble velocities, starting at 3 cm s^{-1} and peaking at around 7 cm s^{-1}. This could partly explain the very low cleaning efficiency of surfaces soiled by the *Bacillus cereus* 98/4 spores by the best foam cleaning conditions observed for *B. amyloliquefaciens*. *B. cereus* spores presented a high contact angle value (111.1°) as described recently (Faille et al., 2019a), largely over the value of 59° for the hydrophobic particles deduced from the bell-shaped curve (Kondjoyan et al., 2009b). With *B. cereus* spores, greater foam velocities should be tested, while conserving the bubble pattern obtained in this work under 1D flow conditions.

Time-variations relating to the capillary forces as an inlet condition in a modified adhesion and dynamic model were suggested as a way of predict the nano- and micro-movements of particles during their detachment from a surface (Kondjoyan et al., 2009). These movements are probably emphasized by the shear force fluctuations in our experimental conditions, which differ greatly to capillary flow conditions.

Conclusions and perspectives

This work constitutes a cornerstone for future work on the implementation of foam flow cleaning in the industry. This requires further activities on foam flow characterisation in order to be able to design a new efficient cleaning foam structure e.g. less drainage phenomenon and increase of the wall shear stress at the bottom of the ducts, which would take into account the surfactant used (more profitable and usable industrially) than the SDS and the temperature of the foam. The decrease of the temperatures seemed to play a significant role in its cohesion strengths (data not shown) potentially corresponding to food processing sectors working under positive cold conditions e.g. fresh-cut or frozen vegetable

and fruit industries. The novelty of this concept is to clean complex equipment while using far less potable water, at a lower energy consumption level.

Acknowledgments

This work was supported by the project Veg-I-Tec (programme Interreg V France-Wallonia-Flanders GoToS3), ANIOS laboratories and the European Regional Development fund via the Hauts-de-France region.

References

Benezech, T., Faille, C., 2018. Two-phase kinetics of biofilm removal during CIP. Respective roles of mechanical and chemical effects on the detachment of single cells vs cell clusters from a Pseudomonas fluorescens biofilm. J. Food Eng. 219, 121–128. https://doi.org/10.1016/j.jfoodeng.2017.09.013

Blel, W., Legentilhomme, P., Bénézech, T., Fayolle, F., 2013. Cleanabilty study of a Scraped Surface Heat Exchanger. Food and Bioproducts Processing 91, 95–102. https://doi.org/10.1016/j.fbp.2012.10.002

Blel, W., Legentilhomme, P., Le Gentil-Lelièvre, C., Faille, C., Legrand, J., Bénézech, T., 2010. Cleanability study of complex geometries: Interaction between B. cereus spores and the different flow eddies scales. Biochemical Engineering Journal 49, 40–51. https://doi.org/10.1016/j.bej.2009.11.009

Bretherton, F.P., 1961. The motion of long bubbles in tubes. Journal of Fluid Mechanics 10, 166. https://doi.org/10.1017/S0022112061000160

Chovet, R., 2015. Experimental and numerical characterization of the rheological behavior of a complex fluid: application to a wet foam flow through a horizontal straight duct with and without flow disruption devices (FDD). Université de Valenciennes et du Hainaut-Cambresis.

Chovet, R., Aloui, F., 2016. Liquid Film Thickness: Study and Influence over Aqueous Foam Flow. J. Appl. Fluid Mech. 9, 39–48.

Chovet, R., Aloui, F., Keirsbulck, L., 2014. Gas-Liquid Foam Through Straight Ducts and Singularities: CFD Simulations and Experiments. https://doi.org/10.1115/FEDSM2014-21190

Cunault, C., Faille, C., Briandet, R., Postollec, F., Desriac, N., Benezech, T., 2018. Pseudomonas sp. biofilm development on fresh-cut food equipment surfaces – a growth curve – fitting approach to building a comprehensive tool for studying surface contamination dynamics. Food and Bioproducts Processing 107, 70–87. https://doi.org/10.1016/j.fbp.2017.11.001

Dallagi, H., Al Saabi, A., Faille, C., Benezech, T., Augustin, W., Aloui, F., 2019. Cfd Simulations of the Rheological Behavior of Aqueous Foam Flow Through a Half-

Sudden Expansion, in: Proceedinge of the Asme/Jsme/Ksme Joint Fluids Engineering Conference, 2019, Vol 1. Amer Soc Mechanical Engineers, New York, p. UNSP V001T01A030.

Dallagi, H., Gheith, R., Al Saabi, A., Faille, C., Augustin, W., Benezech, T., Aloui, F., 2018a. CFD Characterization of a Wet Foam Flow Rheological Behavior, in: Volume 3: Fluid Machinery; Erosion, Slurry, Sedimentation; Experimental, Multiscale, and Numerical Methods for Multiphase Flows; Gas-Liquid, Gas-Solid, and Liquid-Solid Flows; Performance of Multiphase Flow Systems; Micro/Nano-Fluidics. Presented at the ASME 2018 5th Joint US-European Fluids Engineering Division Summer Meeting, ASME, Montreal, Quebec, Canada, p. V003T20A004. https://doi.org/10.1115/FEDSM2018-83338

Dallagi, H., Gheith, R., Al Saabi, A., Faille, C., Augustin, W., Benezech, T., Aloui, F., 2018b. CFD Characterization of a Wet Foam Flow Rheological Behavior, in: Volume 3: Fluid Machinery; Erosion, Slurry, Sedimentation; Experimental, Multiscale, and Numerical Methods for Multiphase Flows; Gas-Liquid, Gas-Solid, and Liquid-Solid Flows; Performance of Multiphase Flow Systems; Micro/Nano-Fluidics. Presented at the ASME 2018 5th Joint US-European Fluids Engineering Division Summer Meeting, ASME, Montreal, Quebec, Canada, p. V003T20A004. https://doi.org/10.1115/FEDSM2018-83338

Dogan, B., Boor, K.J., 2003. Genetic diversity and spoilage potentials among Pseudomonas spp. isolated from fluid milk products and dairy processing plants. Appl. Environ. Microbiol. 69, 130–138.

Faille, C., Bihi, I., Ronse, A., Ronse, G., Baudoin, M., Zoueshtiagh, F., 2016. Increased resistance to detachment of adherent microspheres and Bacillus spores subjected to a drying step. Colloids and Surfaces B: Biointerfaces 143, 293–300. https://doi.org/10.1016/j.colsurfb.2016.03.041

Faille, C., Cunault, C., Dubois, T., Benezech, T., 2018. Hygienic design of food processing lines to mitigate the risk of bacterial food contamination with respect to environmental concerns. Innov. Food Sci. Emerg. Technol. 46, 65–73. https://doi.org/10.1016/j.ifset.2017.10.002

Faille, C., Lemy, C., Allion-Maurer, A., Zoueshtiagh, F., 2019. Evaluation of the hydrophobic properties of latex microspheres and Bacillus spores. Influence of the particle size on the data obtained by the MATH method (microbial adhesion to hydrocarbons). Colloid Surf. B-Biointerfaces 182, UNSP 110398. https://doi.org/10.1016/j.colsurfb.2019.110398

Faille, C., Lequette, Y., Ronse, A., Slomianny, C., Garénaux, E., Guerardel, Y., 2010. Morphology and physico-chemical properties of Bacillus spores surrounded or not with an exosporiumConsequences on their ability to adhere to stainless steel. International Journal of Food Microbiology 143, 125–135. https://doi.org/10.1016/j.ijfoodmicro.2010.07.038

Gahleitner, B., Loderer, C., Fuchs, W., 2013. Chemical foam cleaning as an alternative for flux recovery in dynamic filtration processes. Journal of Membrane Science 431, 19–27. https://doi.org/10.1016/j.memsci.2012.12.047

552 Geeraerd, A.H., Valdramidis, V.P., Van Impe, J.F., 2005. GInaFiT, a freeware tool to assess
553 non-log-linear microbial survivor curves. International Journal of Food Microbiology
554 102, 95–105. https://doi.org/10.1016/j.ijfoodmicro.2004.11.038
555 Jullien, C., Benezech, T., Gentil, C.L., Boulange-Petermann, L., Dubois, P.E., Tissier, J.P.,
556 Traisnel, M., Faille, C., 2008. Physico-chemical and hygienic property modifications
557 of stainless steel surfaces induced by conditioning with food and detergent.
558 Biofouling 24, 163–172. https://doi.org/10.1080/08927010801958960
559 Kondjoyan, A., Dessaigne, S., Herry, J.-M., Bellon-Fontaine, M.-N., 2009a. Capillary force
560 required to detach micron-sized particles from solid surfaces—Validation with
561 bubbles circulating in water and 2μm-diameter latex spheres. Colloids and Surfaces
562 B: Biointerfaces 73, 276–283. https://doi.org/10.1016/j.colsurfb.2009.05.022
563 Li, G., Tang, L., Zhang, X., Dong, J., 2019. A review of factors affecting the efficiency of
564 clean-in-place procedures in closed processing systems. Energy 178, 57–71.
565 https://doi.org/10.1016/j.energy.2019.04.123
566 Mai, Z., Butin, V., Rakib, M., Zhu, H., Rabiller-Baudry, M., Couallier, E., 2016. Influence
567 of bulk concentration on the organisation of molecules at a membrane surface and
568 flux decline during reverse osmosis of an anionic surfactant. J. Membr. Sci. 499, 257–
569 268. https://doi.org/10.1016/j.memsci.2015.10.012
570 Moerman, F., Rizoulières, P., Majoor, F.A., 2014. 10 - Cleaning in place (CIP) in food
571 processing, in: Lelieveld, H.L.M., Holah, J.T., Napper, D. (Eds.), Hygiene in Food
572 Processing (Second Edition). Woodhead Publishing, pp. 305–383.
573 https://doi.org/10.1533/9780857098634.3.305
574 Peng, J.-S., Tsai, W.-C., Chou, C.-C., 2002. Inactivation and removal of Bacillus cereus by
575 sanitizer and detergent. Int. J. Food Microbiol. 77, 11–18.
576 Pietrysiak, E., Kummer, J.M., Hanrahan, I., Ganjyal, G.M., 2019. Efficacy of Surfactant
577 Combined with Peracetic Acid in Removing Listeria innocua from Fresh Apples. J.
578 Food Prot. 82, 1959–1972. https://doi.org/10.4315/0362-028X.JFP-19-064
579 Ribeiro, M.C.E., Fernandes, M. da S., Kuaye, A.Y., Gigante, M.L., 2019. Influence of
580 different cleaning and sanitisation procedures on the removal of adhered Bacillus
581 cereus spores. Int. Dairy J. 94, 22–28. https://doi.org/10.1016/j.idairyj.2019.02.011
582 Srey, S., Jahid, I.K., Ha, S.-D., 2013. Biofilm formation in food industries: A food safety
583 concern. Food Control 31, 572–585. https://doi.org/10.1016/j.foodcont.2012.12.001
584 Tauveron, G., Slomianny, C., Henry, C., Faille, C., 2006. Variability among Bacillus cereus
585 strains in spore surface properties and influence on their ability to contaminate food
586 surface equipment. Int. J. Food Microbiol. 110, 254–262.
587 https://doi.org/10.1016/j.ijfoodmicro.2006.04.027
588 Tisné, P., Aloui, F., Doubliez, L., 2003. Analysis of wall shear stress in wet foam flows using
589 the electrochemical method. International Journal of Multiphase Flow 29, 841–854.
590 https://doi.org/10.1016/S0301-9322(03)00038-7
591 Tisné, P., Doubliez, L., Aloui, F., 2004. Determination of the slip layer thickness for a wet
592 foam flow. Colloids and Surfaces A: Physicochemical and Engineering Aspects 246,
593 21–29. https://doi.org/10.1016/j.colsurfa.2004.07.014

594

Figure 1. Diagram of foam cleaning in place prototype

Figure 2: Bubble velocities measured at the top and lateral walls of the transparent duct measured at three positions (in red) in relation to the number of generators (one: square, two: diamond, three: triangle) and with the foam qualities (white: 50%, grey: 60% and black: 70%)

Figure 3. Foam visualization at the top wall of the transparent Plexiglas duct just upstream of the test ducts for the three foam qualities and foam flow conditions induced by the generators

Figure 4. Bubble size (mm) pattern; A: one generator, B: 2 generators, C: 3 generators and frequency of bubbles' passage (D) in front of the optical probe at the top wall for the three foam qualities: 0.5 (dark blue), 0.6 (light blue), 07 (yellow)

Figure 5. Removal kinetics of *B. amyloliquefaciens* spores under different flow conditions (mean values): 1 generator (square), 2 generators (diamond), 3 generators (triangle) for the foam qualities of 50% (A), 60% (B) and 70% (C); Removal kinetics with the foam quality of 50%, one generator compared to CIP ("foam quality" being equal to zero in that case) (D)

Figure 6. Decimal reduction of the *Bacillus amyloliquefaciens* spores induced by different flow conditions at 20 min cleaning time: comparison of the combined effects of the flow conditions and the foam quality including CIP conditions

Figure 7. Variations induced by the combination of the foam quality (including CIP conditions for the last two graphs) and the flow rate induced by one, two or three generators on the kinetics parameters f, Kmax1 and Kmax2. According to the Tukey grouping, letters were indicated with potentially three classes A, AB and B; common letters meaning no significant differences

Figure 8. Comparison between the removal of *Bacillus amyloliquefaciens* and *Bacillus cereus* spores: cleaning with foam of β=50% and one generator

Figure 9. Observations of the stainless steel coupon contamination before cleaning and after 15 s, 3 min and 20 min with a foam quality of β=50% using one generator or with CIP

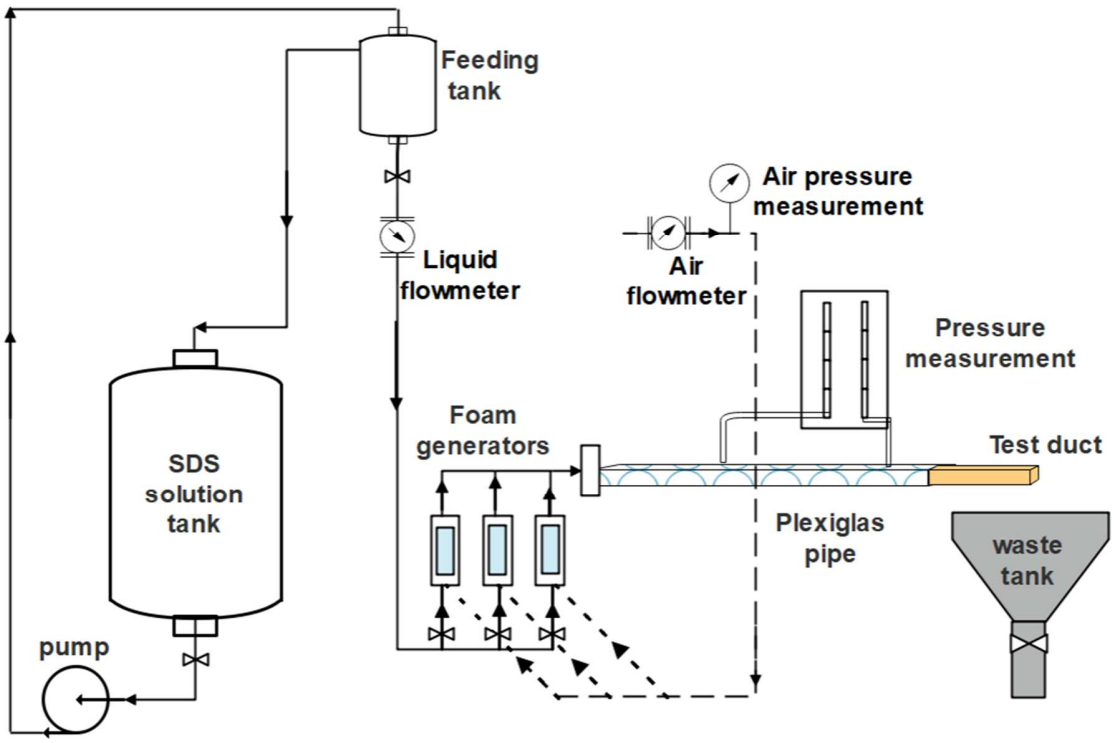
Feeding tank
Air pressure measurement
Liquid flowmeter
Air flowmeter
Pressure measurement
SDS solution tank
Foam generators
Test duct
Plexiglas pipe
waste tank
pump

Top wall **Lateral wall**

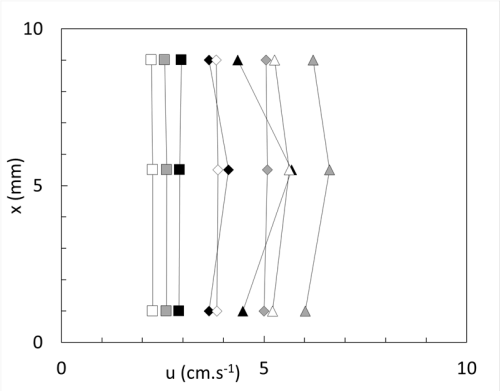

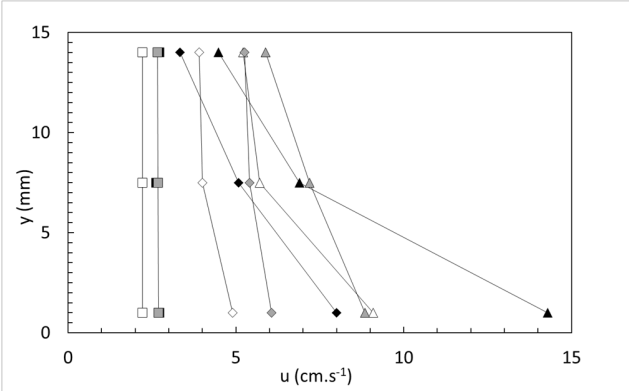

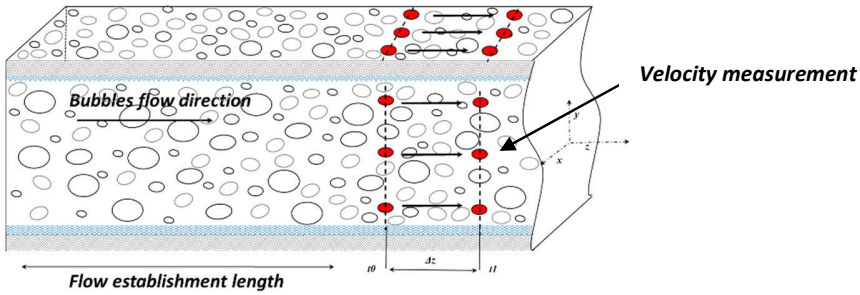

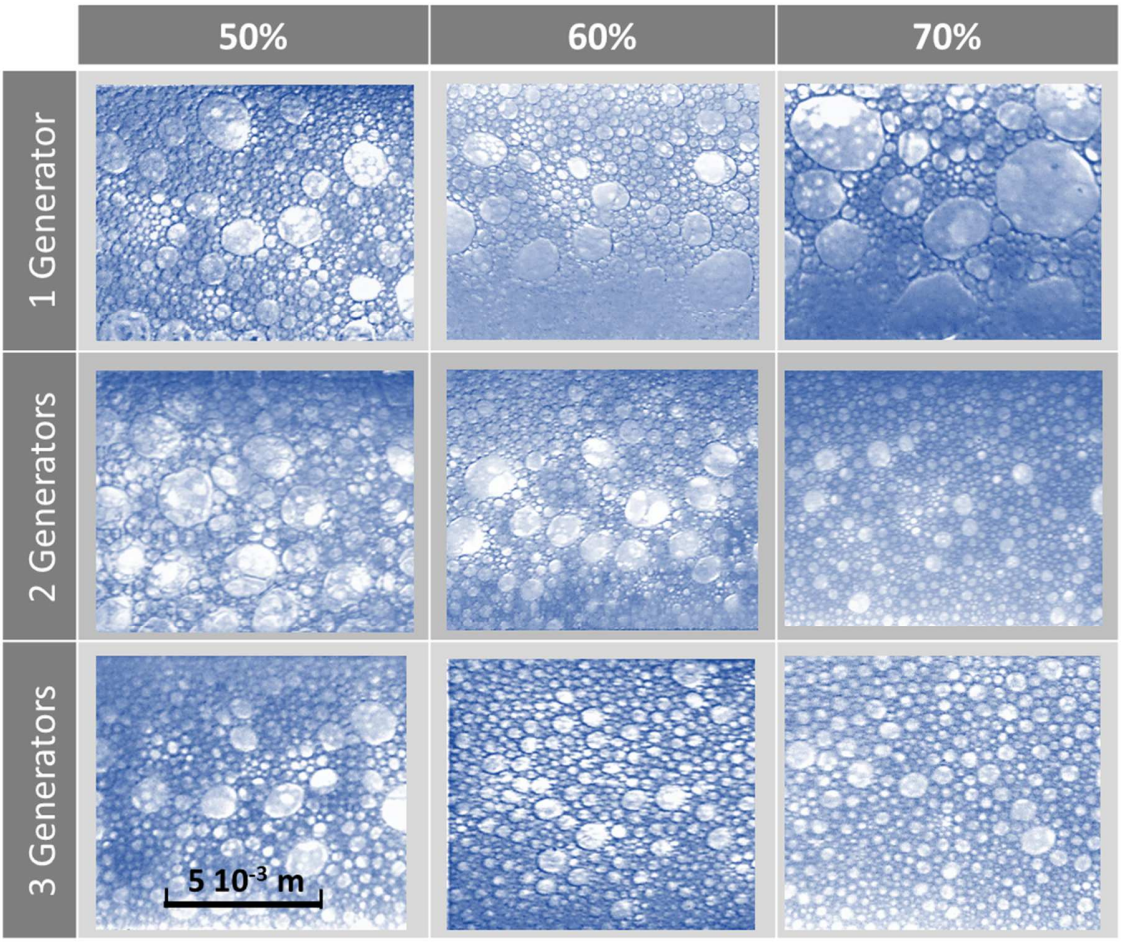
50%
60%
70%
1 Generator
2 Generators
3 Generators
5 10-3 m

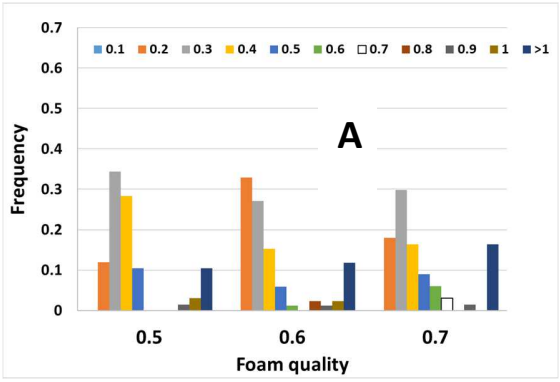
0.1 0.2 0.3 0.4 0.5 0.6 0.7 0.8 0.9 1 >1
A
Frequency
0.7
0.6
0.5
0.4
0.3
0.2
0.1
0
0.5
0.6
0.7
Foam quality

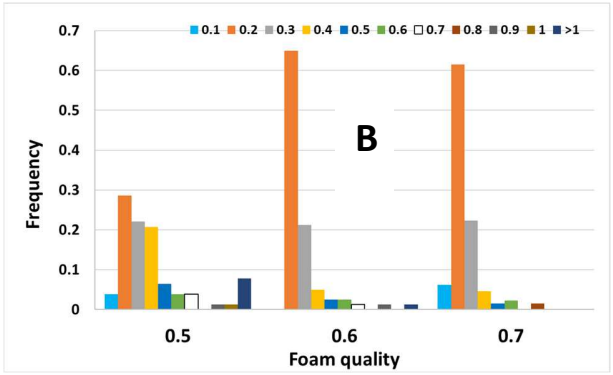
0.1 0.2 0.3 0.4 0.5 0.6 0.7 0.8 0.9 1 >1
B
Frequency
0.7
0.6
0.5
0.4
0.3
0.2
0.1
0
0.5
0.6
0.7
Foam quality

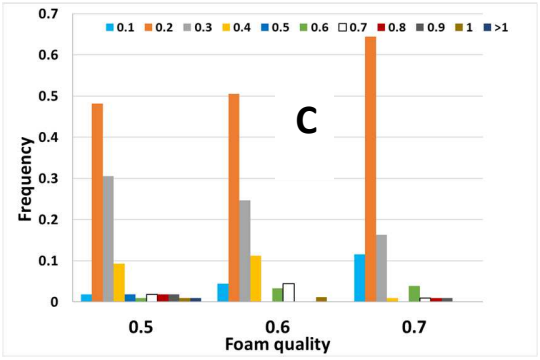
0.1 0.2 0.3 0.4 0.5 0.6 0.7 0.8 0.9 1 >1
C
Frequency
0.7
0.6
0.5
0.4
0.3
0.2
0.1
0
0.5
0.6
0.7
Foam quality

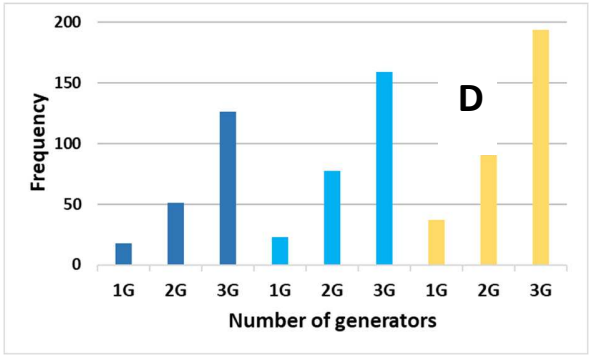
D
Frequency
200
150
100
50
0
1G 2G 3G 1G 2G 3G 1G 2G 3G
Number of generators

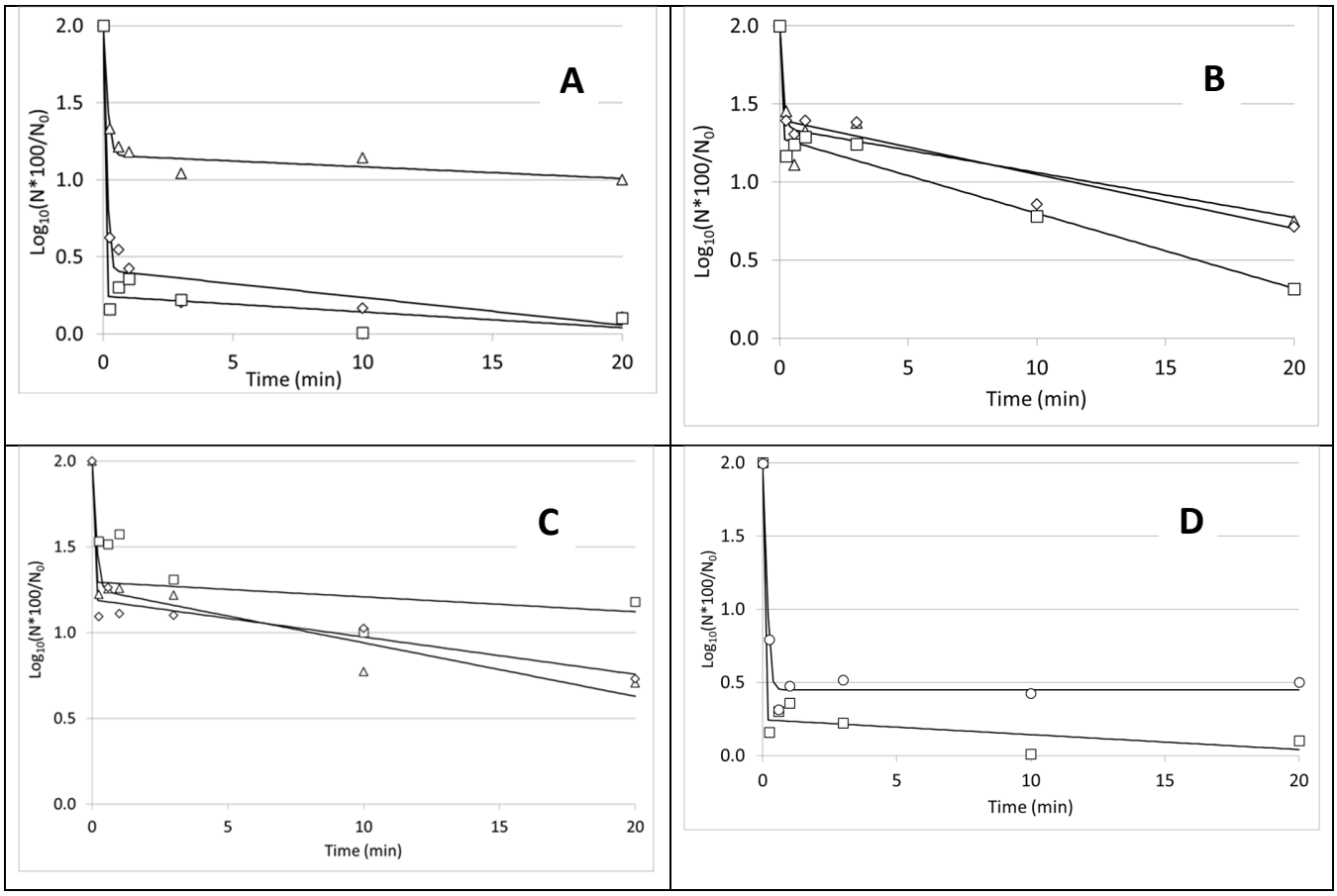
A
B
C
D
Log10(N*100/N0)
Time (min)
0.0
0.5
1.0
1.5
2.0
0
5
10
15
20

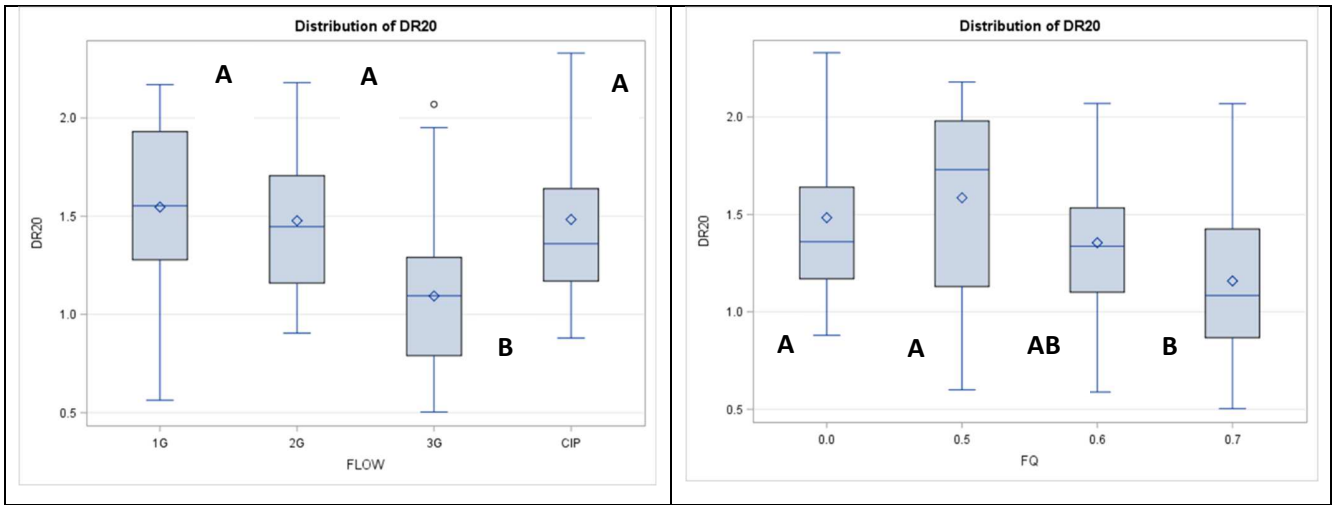
Distribution of DR20
DR20
2.0
1.5
1.0
0.5
A
A
B
A
1G
2G
3G
CIP
FLOW
Distribution of DR20
DR20
2.0
1.5
1.0
0.5
A
A
AB
B
0.0
0.5
0.6
0.7
FQ

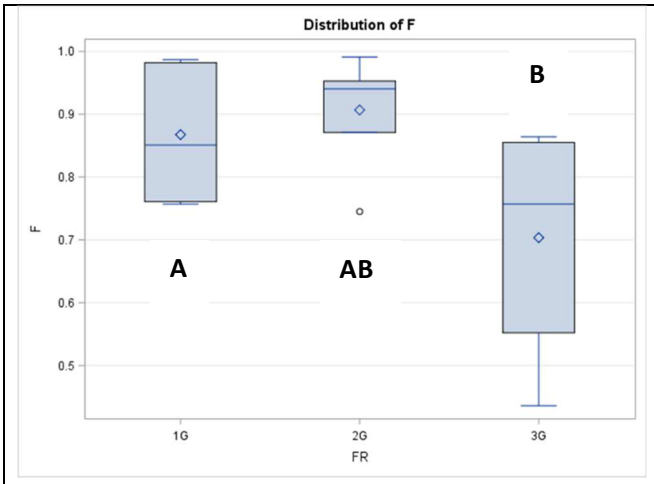
Distribution of F
F
1.0
0.9
0.8
0.7
0.6
0.5
A
AB
B
1G
2G
3G
FR

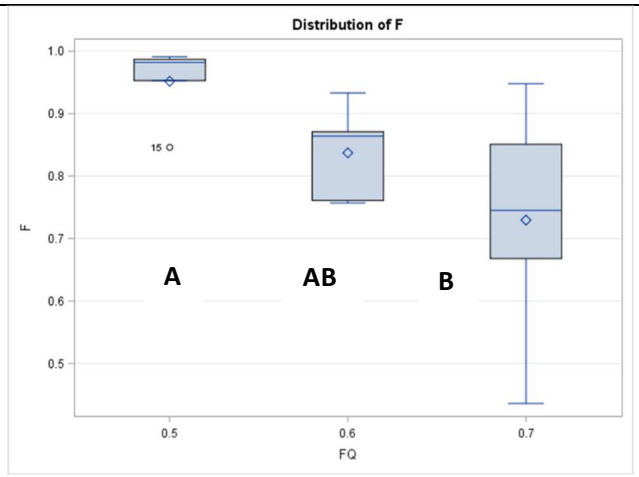
Distribution of F
F
1.0
0.9
0.8
0.7
0.6
0.5
15
A
AB
B
0.5
0.6
0.7
FQ

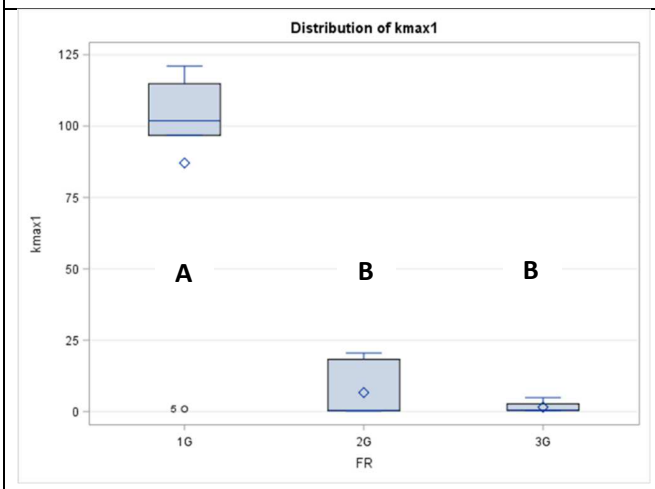
Distribution of kmax1
kmax1
125
100
75
50
25
0
5
A
B
B
1G
2G
3G
FR

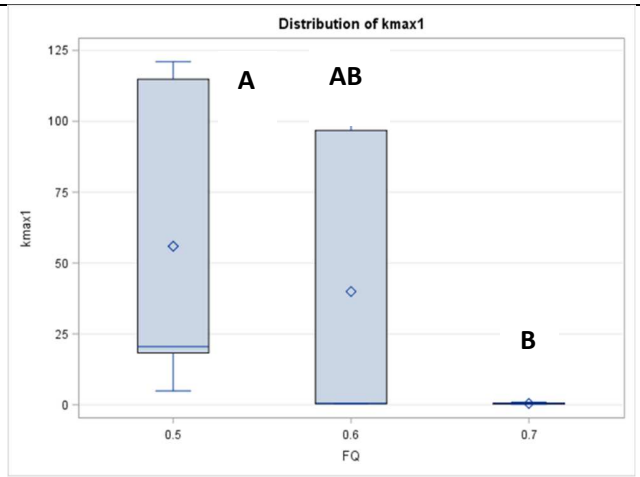
Distribution of kmax1
kmax1
125
100
75
50
25
0
A
AB
B
0.5
0.6
0.7
FQ

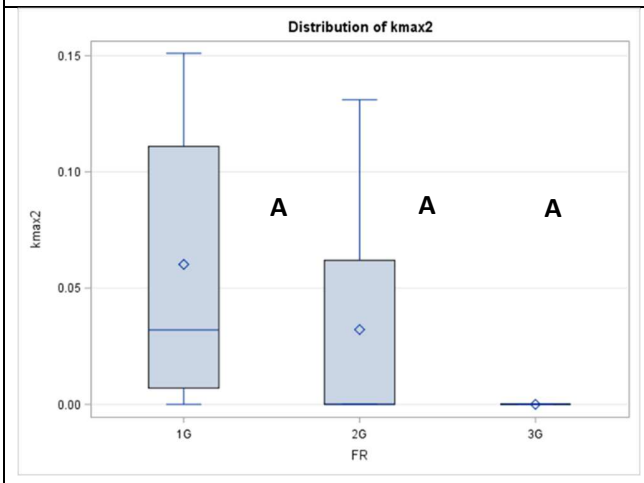
Distribution of kmax2
kmax2
0.15
0.10
0.05
0.00
A
A
A
1G
2G
3G
FR

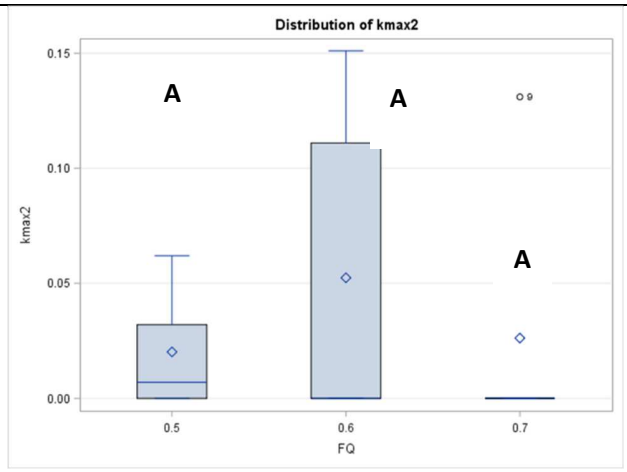
Distribution of kmax2
kmax2
0.15
0.10
0.05
0.00
A
A
A
0.5
0.6
0.7
FQ

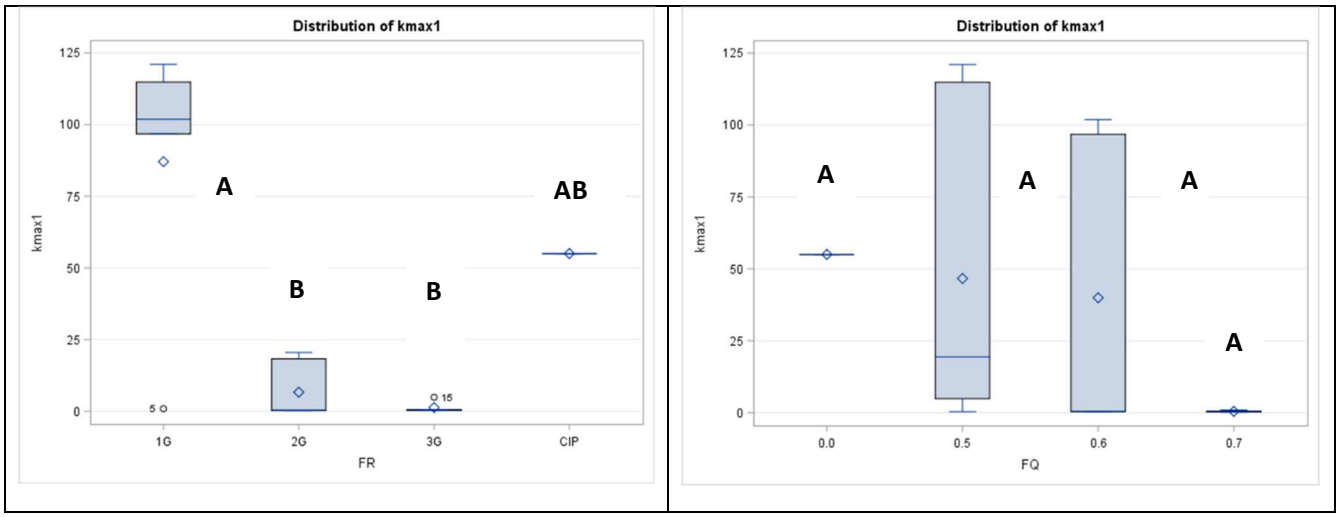
Distribution of kmax1
kmax1
125
100
75
50
25
0
5
15
A
B
B
AB
1G
2G
3G
CIP
FR
Distribution of kmax1
kmax1
125
100
75
50
25
0
A
A
A
A
0.0
0.5
0.6
0.7
FQ

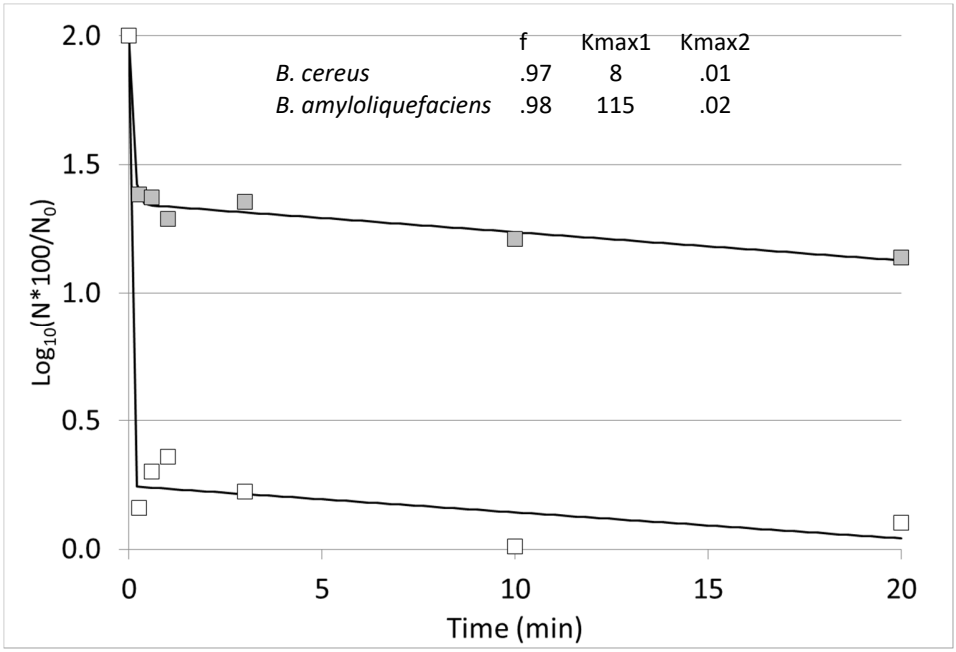
f Kmax1 Kmax2
B. cereus .97 8 .01
B. amyloliquefaciens .98 115 .02
2.0
1.5
1.0
0.5
0.0
Log10(N*100/N0)
0
5
10
15
20
Time (min)

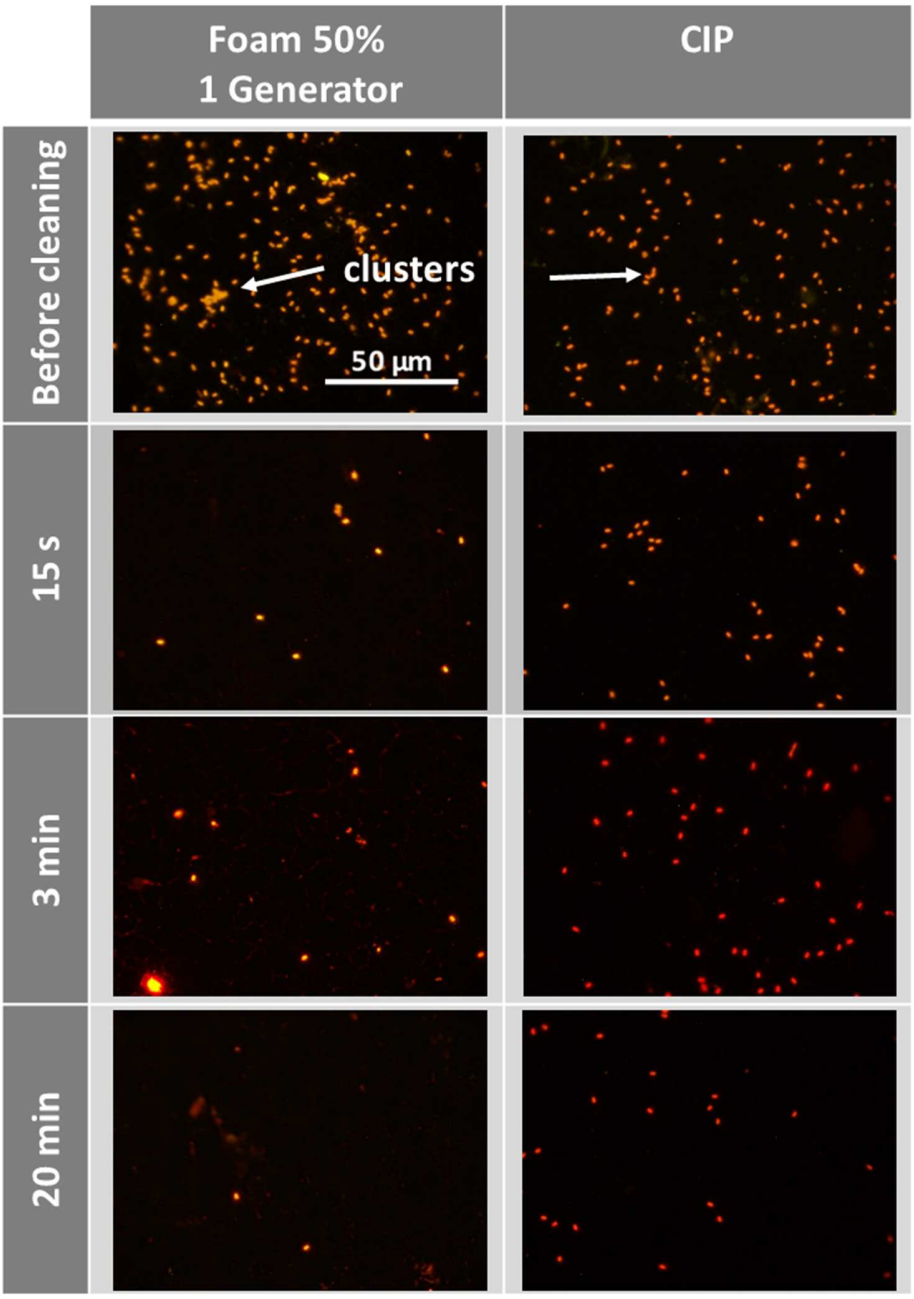
Foam 50%
1 Generator
CIP
Before cleaning
15 s
3 min
20 min
clusters
50 µm

Liquid flow rate ($l.h^{-1}$)	Air flow rate ($l.h^{-1}$)	Foam quality β	Mean velocity ($cm.s^{-1}$)	$\bar{\tau}w$ (Pa)	Re
6	6		2.0	2.2	43
9	9	50%	4.0	4.2	87
13.5	13.5		6.1	5.9	130
4.2	6.3		2.4	2.2	51
8.4	12.6	60%	4.9	4.4	101
12.6	18.9		7.3	6.0	151
4.2	9.8		2.9	2.4	67
8.4	19.6	70%	5.7	5.1	135
12.6	29.4		8.6	6.4	202
650	-	0 (no foam)	120	5.1	14500

Table 1. Flow conditions for the foam flow and the CIP (foam quality = 0)